International Conference KNOWLEDGE-BASED ORGANIZATION
Vol. XXXI No 3 2025

STUDY FOR A 122 mm ARTILLERY ROCKET STEERED WITH LATERAL THRUSTERS

Marius-Ionuț MĂRMUREANU

Military Equipment and Technologies Research Agency, Clinceni, Romania
mmarmureanu@acttm.ro

Abstract: *The article analyses how lateral correction thrusters can reduce impact point dispersion for a 122 mm artillery rocket. The rocket is assumed to be equipped with a control unit consisting of 36 solid propellant lateral thrusters. A six-degree-of-freedom (6-DOF) mathematical model of the rocket's external ballistics was employed to study the effects of various parameters on accuracy across different launch elevation angles. The findings indicate that implementing control algorithms significantly improves the rocket's accuracy by decreasing the dispersion of the impact points. A key observation from the initial qualitative evaluation is the importance of timing in the activation of the thrusters. Specifically, the results suggest that the lateral thrusters should be triggered shortly after the solid rocket motor finishes its burn phase. This early activation appears crucial to maximizing the effectiveness of the trajectory corrections. Overall, the study demonstrates the potential of integrated control systems to enhance the precision of unguided artillery rockets through real-time trajectory adjustments.*

Keywords: rocket artillery, pulse jet control, lateral thruster

1. Introduction

The concept of using lateral thrusters to reduce the dispersion of slowly rotating unguided rockets has its origins in the pioneering work of American researchers Harkins and Brown [1], who are credited with developing this innovative idea. Their work, which became the subject of a patent, introduced an active damping system aimed at improving the accuracy of unguided artillery rockets. This technical solution involved a cylindrical gas-dynamic module, consisting of eight lateral thrusters. Four of these thrusters provided a total impulse of 4 N·s each, while the remaining four offered 1 N·s each. The module was designed to be inserted into the unguided rocket's body at a distance of six calibres from the nose cone. By activating these lateral thrusters, the system could effectively correct the rocket's trajectory during flight, reducing its impact point dispersion, especially for those rockets prone to yaw and pitch instability due to rotation.

In parallel, Jitpraphai and Costello [2, 3] made significant contributions to this field. Their work extended the concept to the use of 32 lateral thrusters, arranged radially around the rocket's body. These thrusters were positioned 0.24 meters from the rocket's nose cone, and their total impulse ranged between 5 N·s [3] and 20 N·s [2]. In their study, the duration of action for each thruster was maintained at 0.01 seconds. By using these lateral thrusters, Jitpraphai and Costello demonstrated a reduction in the dispersion of impact points, further validating the potential of lateral thrust

DOI: 10.2478/kbo-2025-0084

systems to correct trajectory errors in unguided rockets.

Gupta [4, 5] later expanded on this research, focusing on the 122 mm artillery rocket. In Gupta's study, the configuration consisted of 32 lateral thrusters placed 0.382 meters from the rocket's nose cone. After performing numerical evaluations, Gupta identified the optimal configuration, which required each thruster to provide a total impulse of 10 N·s. This study helped refine the understanding of how lateral thrusters could be used effectively to enhance the accuracy of artillery rockets, providing a more stable and predictable flight path.

Building on these developments, Pavkovic [6, 7] applied this technology to indirect firing with the 262 mm M-87 Orkan unguided artillery rocket, a larger system with different flight dynamics. For the Orkan rocket, Pavkovic [6] proposed using 32 small solid propellant lateral thrusters, each delivering 15 N·s of impulse over 0.005 seconds. In another configuration, Pavkovic [7] suggested using 35 lateral thrusters, each providing a more substantial impulse of 70 N·s. These variations in impulse and action duration were explored to determine their impact on trajectory correction and overall accuracy, marking another advancement in the application of lateral thrusters.

Gao [8] further contributed to the field with a study on the 122 mm artillery rocket equipped with extended range capabilities. In his model, Gao utilized 50 solid propellant lateral thrusters, each delivering 15 N·s of total impulse with a firing duration of 0.02 seconds. These thrusters were positioned 0.869 meters from the rocket's nose cone. Gao's work highlighted how the inclusion of additional thrusters, with carefully optimized thrust profiles and activation durations, could further improve the performance of extended-range artillery rockets, enabling more precise control over their flight paths and reducing the potential for accuracy degradation over long distances.

Another influential study in this area was conducted by Jacewicz [9], who focused on the 122 mm artillery rocket with extended range. Jacewicz's configuration involved 30 lateral thrusters, placed at 1.9 meters from the base of the rocket. Each thruster in this model was designed to provide thrust forces ranging from 200 to 1000 N, with an activation duration of 0.02 seconds. By varying the thrust levels and the duration of action, Jacewicz's study provided insights into the balance between correction precision and the energy required for thruster activation, contributing valuable data for optimizing the use of lateral thrusters in extended-range artillery rockets.

Glebocki [10], in turn, studied the existing 160 mm artillery rocket, which presented unique challenges due to its size and operational characteristics. Glebocki's configuration consisted of 34 identical lateral thrusters placed 2.16 meters from the base of the rocket. These thrusters were designed to operate for 0.04 seconds, with thrust amplitudes ranging from 100 N to 2000 N. The wide range of thrust levels was intended to explore the effects of different impulse magnitudes on the rocket's trajectory, aiming to identify configurations that would ensure optimal accuracy across a variety of launch conditions.

Ozog [11] conducted research on modifying the configuration of the 128 mm artillery rocket, focusing on the integration of lateral thrusters for enhanced control. This configuration included 30 small solid propellant thrusters, each located 2.03 meters from the rocket base. These thrusters operated for 0.02 seconds, delivering a maximum thrust of 900 N. Ozog's study explored the trade-offs between thruster number, placement, and thrust levels, contributing to a more comprehensive understanding of how these variables could be manipulated to improve the stability and accuracy of medium-calibre rockets.

In more recent studies, Jacewicz [12] examined the use of lateral thrusters for a short-range 122 mm artillery rocket. In this configuration, 32 correction thrusters were employed, each generating a thrust of 200 N and having a burn time of 0.03 seconds. This work focused on fine-tuning the trajectory correction system for shorter-range rockets, which have different aerodynamic characteristics compared to longer-range systems.

Miedzinski also conducted investigations into the short 122 mm artillery rocket, utilizing a control module consisting of 32 small solid propellant lateral thrusters. Each thruster in Miedzinski's study operated for 0.05 seconds and generated a thrust of 800 N [13]. This research contributed to refining the parameters for short-range rocket systems, with a focus on providing precise control over the rocket's trajectory during flight, ultimately leading to better accuracy in field conditions.

2. The mathematical model of the general motion equations in the Tait-Bryan formulation

The mathematical model that defines general motion in the Tait-Bryan formulation consists of a system of 12 first-order differential equations. Half of these, called dynamic equations, are obtained based on the momentum theorem and the angular momentum theorem applied to a body of variable mass. The other half, called kinematic equations, describe on the one hand the relationship between the components of the velocity vector of the centre of mass expressed in the inertial trihedron and in the artillery rocket trihedron (u, v and w), and on the other hand the relationship between the components of the rotational velocity around the centre of mass (p, q and r) associated with the artillery rocket trihedron and the derivatives of the Euler attitude angles. Euler angles are used to describe the orientation of the mobile trihedron connected to the artillery rocket with respect to the inertial trihedron: ψ – heading angle (direction or course angle), θ – longitudinal attitude (pitch angle) and ϕ – lateral inclination (roll angle).

The main reference systems (*Figure 1*) used in the development of kinematic equations are the following:

i) $O_0X_0Y_0Z_0$ – the initial starting trihedron (inertial trihedron) with a fixed origin, located at sea level, where the axis O_0X_0 is horizontally oriented, and the axis O_0Z_0 is oriented upwards vertically;

ii) $O_0X_gY_gZ_g$ – the fixed ground trihedron with the origin and O_0X_g axis orientation identical to those of the initial starting trihedron, and the axis O_0Z_g is oriented vertically downwards;

iii) $Ox_gy_gz_g$ – the mobile ground trihedron with a mobile origin, located at the centre of mass of the artillery rocket, the axes being parallel to those of the fixed ground trihedron;

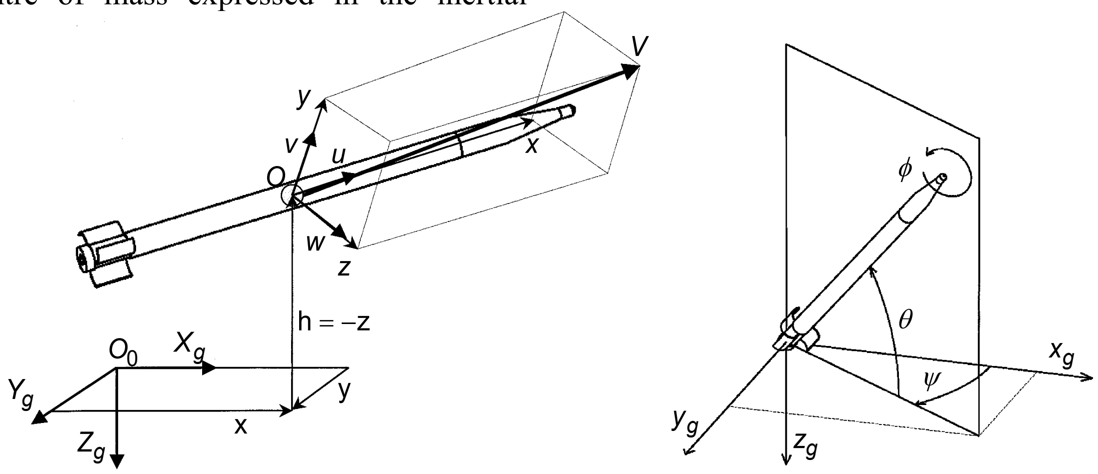

Figure 1: Coordinate systems for the external ballistics model

iv) $Oxyz$ – the rocket (mobile) trihedron with a mobile origin, located at the centre of mass of the artillery rocket; the Ox axis coincides with the axis of symmetry of the configuration, having the direction towards the top of the artillery rocket, and the axes Oy and Oz are perpendicular to the first, respectively to the second plane of symmetry of the artillery rocket.

To develop the mathematical model of the general motion equations of the artillery rocket in the Tait-Bryan formulation, the following forces and moments are considered [14]:

- thrust force;
- aerodynamic force;
- pitch/yaw damping force;
- weight force;
- main aerodynamic moment;
- transverse aerodynamic damping moment (pitch/yaw damping);
- axial aerodynamic moment caused by the tilt of the stabilizer empennage;
- axial aerodynamic damping moment (roll damping);
- axial gas-dynamic damping moment;
- transverse gas-dynamic damping moment.

In the logic of what was presented previously, the equations of general motion in the Tait-Bryan formulation are defined below, with the necessary and obvious mention that all dynamic equations are related exclusively to the artillery rocket trihedron (mobile) [14]:

$$\frac{du}{dt}=\frac{T}{m}-g\sin\theta-\frac{\pi\rho V^2 d^2}{8m}C_X+rv-qw; \tag{1}$$

$$\frac{dv}{dt}=g\sin\phi\cos\theta -\frac{\pi\rho V^2 d^2}{8m}\left(C_{Y_\beta}\beta+C_{Y_r}\frac{d}{2V}r\right)+pw-ru; \tag{2}$$

$$\frac{dw}{dt}=g\cos\phi\cos\theta -\frac{\pi\rho V^2 d^2}{8m}\left(C_{N_\alpha}\alpha+C_{N_q}\frac{d}{2V}q\right)+qu-pv; \tag{3}$$

$$\frac{dp}{dt}=\frac{\pi\rho V^2 d^3}{8I_x}\left(C_{l_\delta}+C_{l_p}\frac{d}{2V}p\right) +\frac{1}{I_x}\left(\frac{dI_x}{dt}+\frac{1}{2}\left|\frac{dm}{dt}\right|r_e^2\right)p; \tag{4}$$

$$\frac{dq}{dt}=\frac{\pi\rho V^2 d^3}{8I_t}\left[C_{m_\alpha}\alpha+\left(C_{m_q}+C_{m_{\dot\alpha}}\right)\frac{d}{2V}q\right] -\frac{1}{I_t}\left\{\frac{dI_t}{dt}+\left|\frac{dm}{dt}\right|\left[\left(l_r-x_{CM}\right)^2+\frac{1}{4}r_e^2\right]\right\}q +\frac{\left(I_t-I_x\right)}{I_t}pr; \tag{5}$$

$$\frac{dr}{dt}=\frac{\pi\rho V^2 d^3}{8I_t}\left[C_{n_\beta}\beta+\left(C_{n_r}r+C_{n_p}p\right)\frac{d}{2V}\right] -\frac{1}{I_t}\left\{\frac{dI_t}{dt}+\left|\frac{dm}{dt}\right|\left[\left(l_r-x_{CM}\right)^2+\frac{1}{4}r_e^2\right]\right\}r +\frac{\left(I_x-I_t\right)}{I_t}pq; \tag{6}$$

$$\frac{d\phi}{dt}=p+q\sin\phi\tan\theta+r\cos\phi\tan\theta; \tag{7}$$

$$\frac{d\theta}{dt}=q\cos\phi-r\sin\phi; \tag{8}$$

$$\frac{d\psi}{dt}=\frac{1}{\cos\theta}\left(q\sin\phi+r\cos\phi\right); \tag{9}$$

$$\frac{dx}{dt}=u\cos\theta\cos\psi +v\left(\sin\phi\sin\theta\cos\psi-\cos\phi\sin\psi\right) +w\left(\cos\phi\sin\theta\cos\psi+\sin\phi\sin\psi\right); \tag{10}$$

$$\frac{dy}{dt}=u\cos\theta\sin\psi +v\left(\sin\phi\sin\theta\sin\psi+\cos\phi\cos\psi\right) +w\left(\cos\phi\sin\theta\sin\psi-\sin\phi\cos\psi\right); \tag{11}$$

$$\frac{dz}{dt}=u\sin\theta-v\sin\phi\cos\theta-w\cos\phi\cos\theta, \tag{12}$$

where $V=\sqrt{u^2+v^2+w^2}$ is the artillery rocket velocity in the mobile trihedron, $\alpha=\arctan\frac{w}{u}$ is the angle of attack, and $\beta=\arcsin\frac{v}{V}$ is the slip (glissade) angle.

3. Gas-dynamic trajectory correction algorithm

The trajectory tracking system in the gas-dynamic guidance module (*Figure 2*) compares the measured coordinates of the artillery rocket $(\hat{x}, \hat{y}, \hat{z})$ with those of the reference trajectory (x_C, x_C, x_C), to define the position error of the rocket in the inertial trihedron.

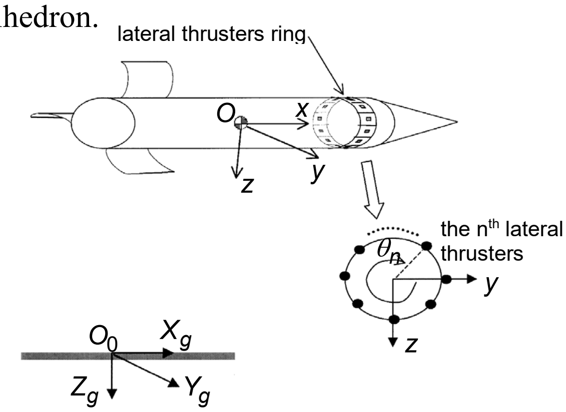

Figure 2: Schematic diagram for artillery rocket with gas-dynamic steering module consisting of lateral thrusters

On the other hand, the artillery rocket position error is converted into the rocket (mobile) trihedron with the following equation:

$$e_x = (x_c - \hat{x})\cos\hat{\theta}\cos\hat{\psi} + (y_c - \hat{y})\cos\hat{\theta}\sin\hat{\psi} + (z_c - \hat{z})\sin\hat{\theta}; \quad (13)$$

$$e_y = (x_c - \hat{x})\left(\sin\hat{\phi}\sin\hat{\theta}\cos\hat{\psi} - \cos\hat{\phi}\sin\hat{\psi}\right) + (y_c - \hat{y})\left(\sin\hat{\phi}\sin\hat{\theta}\sin\hat{\psi} + \cos\hat{\phi}\cos\hat{\psi}\right) - (z_c - \hat{z})\sin\hat{\phi}\cos\hat{\theta}; \quad (14)$$

$$e_z = (x_c - \hat{x})\left(\cos\hat{\phi}\sin\hat{\theta}\cos\hat{\psi} + \sin\hat{\phi}\sin\hat{\psi}\right) + (y_c - \hat{y})\left(\cos\hat{\phi}\sin\hat{\theta}\sin\hat{\psi} - \sin\hat{\phi}\cos\hat{\psi}\right) - (z_c - \hat{z})\cos\hat{\phi}\cos\hat{\theta}. \quad (15)$$

The magnitude and phase of the position error in the transverse plane of the rocket are $\Gamma = \sqrt{e_y^2 + e_z^2}$ and $\gamma = \tan^{-1}\left(e_z/e_y\right)$.

At each calculation cycle performed in the guidance module, the status of the lateral thrusters is checked. For the firing of one of the lateral thrusters to be desirable, the following conditions shall be met, cumulatively:

i) The magnitude of the position error in the transverse plane of the artillery rocket shall be greater than a specified distance: $\Gamma > e_{thresold}$.
ii) The time elapsed since the last firing of a solid propellant lateral thrusters shall be greater than a specified time duration: $t - t_{initiation} > \Delta t_{thresold}$.
iii) The angle between the phase of the position error in the transverse plane of the artillery rocket and the solid propellant lateral thrusters in the ring must be less than a specified value: $\left|\theta_n - \pi - \gamma + \hat{p}\frac{\Delta_{PL}}{2}\right| < \delta_{thresold}$, if $e_y \geq 0$, and $\left|\theta_n - 2\pi - \gamma + \hat{p}\frac{\Delta_{PL}}{2}\right| < \delta_{thresold}$, if $e_y < 0$, where $\hat{p}$ is the angular velocity of the proper rotation of the rocket, and Δ_{PL} being the burning duration of a single lateral thrusters.
iv) The lateral thrusters under consideration must not have been fired previously.

4. Modelling and simulation of the corrected trajectory

For the purpose of modelling and simulating the corrected trajectory, the general motion equations model is completed with the forces (X_{PL}, Y_{PL}, Z_{PL}) and moments (L_{PL}, M_{PL}, N_{PL}) induced by the lateral thrusters grouped in the gas-dynamic steering module [3]:

$$\begin{Bmatrix} X_{PL} \\ Y_{PL} \\ Z_{PL} \end{Bmatrix} = \sum_{i=1}^{n_{PL}} T_i^{PL} \begin{Bmatrix} 0 \\ -\cos\left[2\pi(i-1)/n_{PL}\right] \\ -\sin\left[2\pi(i-1)/n_{PL}\right] \end{Bmatrix} \quad (16)$$

$$\begin{Bmatrix} L_{PL} \\ M_{PL} \\ N_{PL} \end{Bmatrix} = \sum_{i=1}^{n_{PL}} T_i^{PL} \begin{Bmatrix} 0 \\ \sin\left[2\pi(i-1)/n_{PL}\right](x_{CM} - x_{PL}) \\ -\cos\left[2\pi(i-1)/n_{PL}\right](x_{CM} - x_{PL}) \end{Bmatrix} \quad (17)$$

where T^{PL} is the thrust developed by a single lateral thruster, n_{PL} is the total number of them, x_{PL} being the distance between the lateral thrusters ring and the artillery rocket nose cone.

The main performance and dimensional characteristics of the 122 mm artillery rocket with the mounted gas-dynamic guidance module, the *"subject"* of the trajectory correction algorithm, are listed below:

- the outer diameter of the rocket: 122 mm;
- the length of the rocket: 2.97 m;
- the length of the launcher tube: 3 m;
- the total mass of the rocket: 70.6 kg;
- the mass of the solid propellant: 20.45 kg;
- the operation duration of the solid rocket motor: 1.87 s;
- the specific impulse: 206 s;
- the equivalent diameter of the nozzle exit section: 98 mm;
- the position of the lateral thruster's ring, relative to the rocket nose cone: 0.76 m;
- the position of the centre of mass before launch, relative to the rocket nose cone: 1.429 m;
- the position of the centre of mass after the operation of the solid rocket motor, relative to the rocket nose cone: 1.303 m;
- the moment of inertia relative to the longitudinal axis, before launch: 0.173 kg·m^2;
- the moment of inertia relative to the longitudinal axis, after the operation of the solid rocket motor: 0.122 kg·m^2;
- the moment of inertia relative to the transverse axes, before launch: 37.23 kg·m^2;
- the moment of inertia relative to the transverse axes, after the operation of the solid rocket motor: 28.22 kg·m^2;
- the initial angular speed of rotation: 440 rpm.

The aerodynamic coefficients are estimated using the MISSILE DATCOM 2011 GUI software, and the variation of meteorological parameters with altitude is modelled by the normal ballistic atmosphere.

The modelling and simulation of the disturbed trajectory for the 122 mm M-21-OF unguided rocket, without a braking ring, is performed under the initial conditions induced below:

- launch elevation angle: 808 mils and 815 mils (reference: 811 mils);
- pitch angular velocity: –0.01 rad/s and 0.14 rad/s;
- direction angle: 0.1° and –0.1°;
- yaw angular velocity: 0.025 rad/s and –0.025 rad/s;
- proper roll angular velocity: 427.45 rpm and 418.41 rpm (reference: 440 rpm);
- specific impulse: 203.41 s and 202.33 s (reference: 206 s);
- crosswind speed: 2.74 m/s and –1.62 m/s.

The results obtained after implementing the trajectory correction algorithm ($e_{thresold} = 5$ m, $\Delta t_{thresold} = 0.2$ s, $\delta_{thresold} = 1°$, $n_{PL} = 36$, $I_t^{PL} = 20$ N·s and $\Delta_{PL} = 20$ ms), in the situations of perturbations induced by the initial conditions previously presented, are graphically presented in *Figure 3-8*.

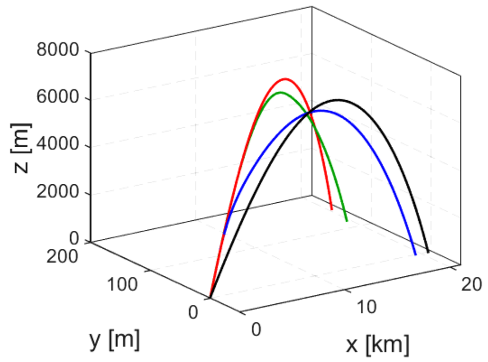

Figure 3: Comparison of 122 mm artillery rocket trajectories

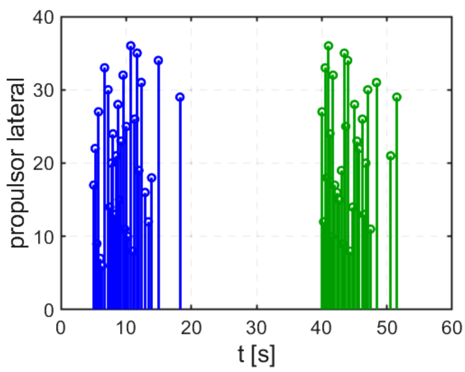

Figure 4: Lateral thrusters firing sequences

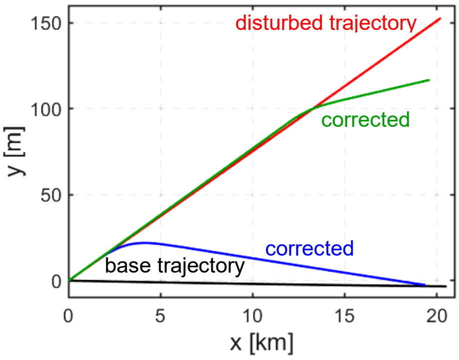

Figure 5: Projection of the trajectory in the horizontal plane

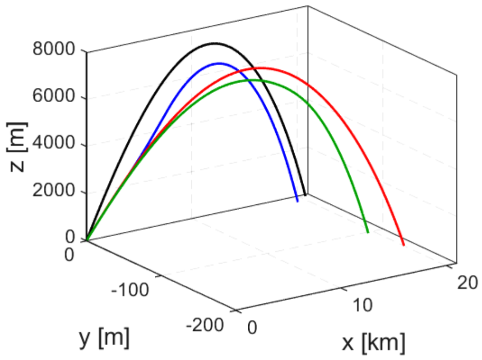

Figure 6: Comparison of 122 mm artillery rocket trajectories

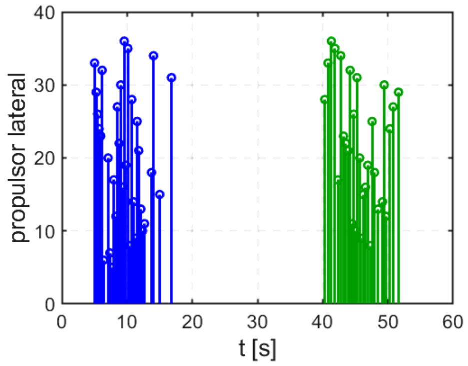

Figure 7: Lateral thrusters firing sequences

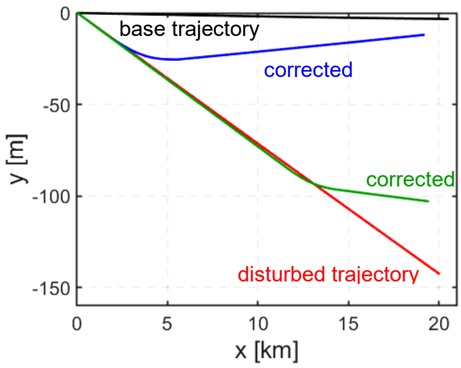

Figure 8: Projection of the trajectory in the horizontal plane

The variation trend induced to the results of the trajectory correction algorithm (especially the deviation in direction) and caused by the modification of the parameters considered important is graphically presented in *Figure 9*.

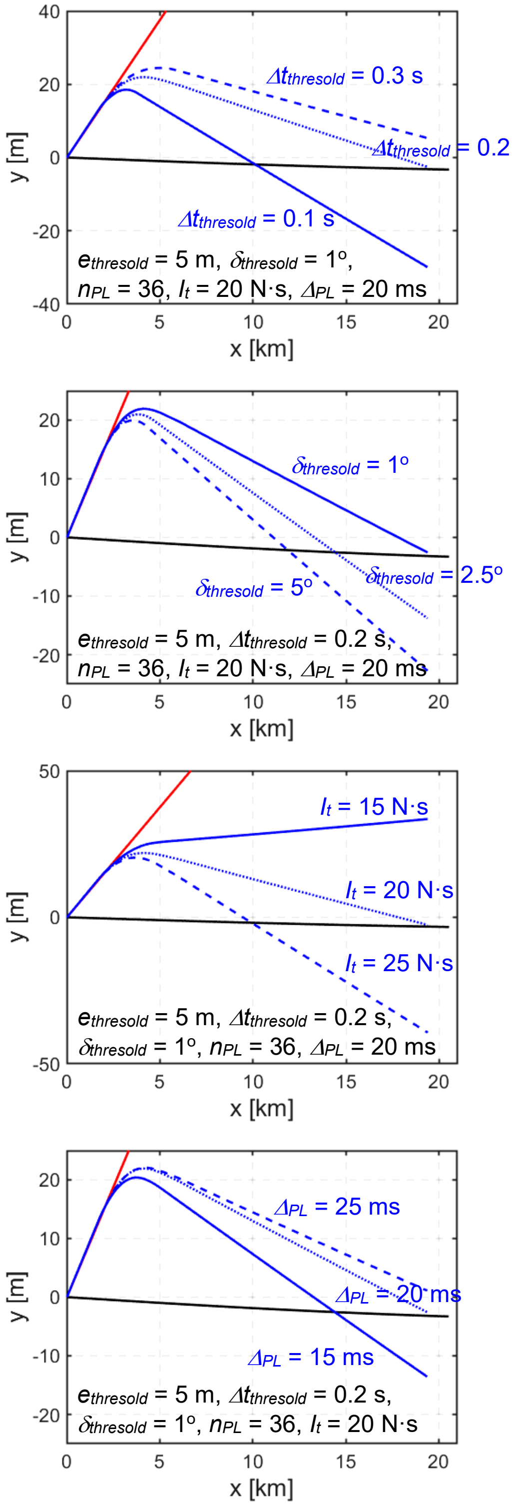

Figure 9: Projection of the trajectory in the horizontal plane

5. Conclusions

A key insight from the initial qualitative evaluation is the critical need to activate the side thrusters shortly after the solid rocket motor ceases combustion. The addition of a 4 kg gas-dynamic guidance module – around 6% of the total mass – significantly increases the 122 mm M-21-OF artillery rocket's mass, while keeping the thrust vector unchanged. This added weight clearly reduces the rocket's maximum range. Consequently, there is a substantial risk that the modified rocket will fall outside the performance parameters defined in current firing tables (TT-74, TT-74m, and TT-74M).

References

[1] Harkins T.E., and Brown T.G. Using Active Damping as a Precision Enhancing Technology for 2.75 inch Rockets, ARL-TR-1772, Army Research Laboratory, USA, 1999.

[2] Jitpraphai T., and Costello M. Dispersion Reduction of a Direct Fire Rocket Using Lateral Pulse Jets, ARL-CR-465, Army Research Laboratory, USA, April 2001.

[3] Jitpraphai T., and Costello M. Dispersion Reduction of a Direct Fire Rocket Using Lateral Pulse Jets, Journal of Spacecraft and Rockets, Vol. 38, No. 6, November-December 2001, pp. 929-936.

[4] Gupta S.K., Saxena S., and Ghosh A.K. On Implementation of Trajectory Correction System on a Routinely Used Artillery Rocket, AIAA 2006-6007, AIAA Atmospheric Flight Mechanics Conference and Exhibit, Keystone, CO, USA, August 21-24, 2006.

[5] Gupta S.K., Saxena S., Singhal A., and Ghosh A.K. Trajectory Correction Flight Control System using Pulsejet on an Artillery Rocket, Defence Science Journal, Vol. 58, No. 1, January 2008, pp. 15-33.

[6] Pavkovic B. Research of Projectile Trajectory Correction Methods in Function of Their Range and Precision Enhancement, PhD thesis, University of Belgrade, Serbia, 2012.

[7] Pavkovic B., Pavic M., and Cuk D. Frequency-Modulated Pulse-Jet Control of an Artillery Rocket, Journal of Spacecraft and Rockets, Vol. 49, No. 2, March-April 2012, pp. 286-294.

[8] Gao M., Zhang Y., and. Yang S. Firing Control Optimization of Impulse Thrusters for Trajectory Correction Projectiles, International Journal of Aerospace Engineering, Vol. 2015, Article ID 781472.

[9] Jacewicz M., Glebocki R., and Ozog R. Monte-Carlo based lateral thruster parameters optimization for 122 mm rocket, In: Conference of Automation, Cham: Springer Nature Switzerland, 2020, pp. 125-134.

[10] Glebocki R., and Jacewicz M. Parametric Study of Guidance of a 160-mm Projectile Steered with Lateral Thrusters, Aerospace, Vol. 7, Iss. 5, May 2020, 61.

[11] Ozog R., Jacewicz M., and Glebocki R. Modified trajectory tracking guidance for artillery rocket, Journal of Theoretical and Applied Mechanics, Vol. 58, No. 3, 2020, pp. 611-622.

[12] Jacewicz M., Lichota P., Miedzinski D., and Glebocki R. Study of Model Uncertainties Influence on the Impact Point Dispersion for a Gasodynamicaly Controlled Projectile, Sensors, Vol. 22, Iss. 9, May 2022, 3257.

[13] Miedzinski D., Glebocki R., and Jacewicz M. Analysis of Sounding Rocket Dispersion Using Monte-Carlo Simulation, In: Conference of Automation, Cham: Springer Nature Switzerland, 2023, pp. 39-50.

[14] Machala D., Dobre S., Albisser M., Gilson M., and Collin F. The Analysis of Vehicle's In-Flight Behaviour Using Quasi-LPV and Nonlinear Models, AIAA Scitech 2019 Forum, San Diego, CA, USA, January 2019.